Physics Letters B 803 (2020) 135355

Contents lists available at ScienceDirect

Physics Letters B

www.elsevier.com/locate/physletb

Many-body effects in (p,pN) reactions within a unified approach

R. Crespo [a,b,*], A. Arriaga [c], R.B. Wiringa [d], E. Cravo [e,c], A. Mecca [a,b], A. Deltuva [f]

[a] Departamento de Física, Instituto Superior Técnico, Universidade de Lisboa, Av. Rovisco Pais 1, 1049-001, Lisboa, Portugal
[b] Centro de Ciências e Tecnologias Nucleares, Universidade de Lisboa, Estrada Nacional 10, 2695-066 Bobadela, Portugal
[c] Departamento de Física, Faculdade de Ciências, Universidade de Lisboa, Campo Grande, 1749-016 Lisboa, Portugal
[d] Physics Division, Argonne National Laboratory, Argonne, IL 60439, USA
[e] Centro de Física Teórica e Computacional, Faculdade de Ciências, Universidade de Lisboa, Campo Grande, 1749-016 Lisboa, Portugal
[f] Institute of Theoretical Physics and Astronomy, Vilnius University, Saulėtekio al. 3, LT-10257 Vilnius, Lithuania

ARTICLE INFO

Article history:
Received 18 June 2019
Received in revised form 4 March 2020
Accepted 5 March 2020
Available online 9 March 2020
Editor: J.-P. Blaizot

Keywords:
Many-body ab initio structure
Correlations
Few-body reaction
(p,pN) reactions
Reduction factors

ABSTRACT

We study knockout reactions with proton probes within a theoretical framework where *ab initio* Quantum Monte Carlo (QMC) wave functions are combined with the Faddeev/Alt-Grassberger-Sandhas few-body reaction formalism. QMC wave functions are used to describe ^{12}C, yielding, for the first time, results consistent with the experimental root mean square (rms) point proton radii, (p,2p) total cross section data, as well as momentum distributions compatible with electron scattering data analysis. In our results for $A \leq 12$ and $(N - Z) \leq 3$ nuclei the ratios between the (i) theoretical cross sections evaluated using QMC and simple Shell Model structure inputs, and (ii) the corresponding ratios between the spectroscopic factors, summed over states below particle emission, are smaller than unity, pointing to the shortcomings of the simple Shell Model. This quenching is more significant for the knockout of the more correlated nucleon of the deficient species. These ratios can be represented reasonably well by a linear combination of the separation energy and the difference between the removed nucleon rms radius in the parent and residual nuclei, showing a mild dependence on these physical quantities.

1. Introduction

The mean field approach to particle systems has played an important role in atomic physics for describing the periodic table of elements and in nuclear physics for explaining many properties of nuclei, such as the origin of the magic numbers leading to additional stability.

Nevertheless, one of the goals of Nuclear Physics is to describe simultaneously, and along the nuclear landscape, nuclear binding, structure, electromagnetic and weak transitions, as well as reactions with electroweak and nuclear probes based on a microscopic description of the interaction between individual nucleons.

A formidable theoretical effort has been performed in developing many-body and cluster approaches to describe nuclei and their application to the study of reactions [1–7]. Strong deviations between these models and simple Shell Model (SM) approaches [9], albeit more sophisticated than the initial mean field models, indicate the presence of non-trivial many-body effects, being interpreted as due to nuclear correlations. Many-body *ab initio* calculations of nuclear structure have demonstrated the need to go beyond the simple SM and to consider models with realistic nucleon-nucleon (NN) and three-nucleon (NNN) interactions. Moreover, explicit NN and NNN correlations have to be built in the wave functions [1,2], which are entirely absent in the simple SM [8,10].

In parallel, for more than 30 years an extensive experimental program, in particular, nucleon knockout reactions with electron and nuclear probes, has been devoted to the study of the shortcomings of the simple SM [11–23]. The interpretation of these reactions has been relying on a standard knockout ansatz based on the assumptions that the knockout/breakup operator does not act on the internal structure of the residual nucleus, making the spectroscopic overlap between the parent and residual nuclei the key nuclear structure input. As a consequence, the cross section can be factorized into the single-particle cross section, defined below, and the corresponding spectroscopic factor (SF) calculated from the squared norm of the overlap function. For (p,pN), this ansatz is supported by the recent work of Ref. [33] where inelastic core excitations give only a small contribution, and by the work of Ref. [34] where an agreement was found between theoretical calculations and experimental results in the case of selected observables such as angular correlations and momentum distributions.

* Corresponding author at: Departamento de Física, Instituto Superior Técnico, Universidade de Lisboa, Av. Rovisco Pais 1, 1049-001, Lisboa, Portugal.
E-mail address: raquel.crespo@tecnico.ulisboa.pt (R. Crespo).

https://doi.org/10.1016/j.physletb.2020.135355

The analysis of earlier (e,e'p) knockout experiments has been used to provide information on the one-nucleon spectroscopic overlaps at low momentum and for low-lying energy states of the residual nucleus. The experimentally extracted SFs were found to be reduced with respect to simple SM ones [11,12].

The nucleon knockout for composite projectiles and target nuclei (called one-nucleon removal in the literature) has been also analyzed extensively [17,18, references therein]. The ratio between the inclusive experimental and the SM theoretical cross sections, R_S, has been found to be below one and to have a strong dependence on the asymmetry parameter ΔS, a measure of the asymmetry of the neutron and proton binding. This has been interpreted as additional correlations in strongly asymmetric (N-Z) systems.

Concurrently, (p,pN) reactions on Oxygen, Carbon and Nitrogen isotopes with $-2 \leq (N-Z) \leq 7$ [19,20,25], and transfer studies of (d,t) and (d,^{3}He) on ^{14,16,18}O [23] and of (p,d) on ^{34,46}Ar [22] have revealed a nearly constant R_S as a function of ΔS.

Theoretical calculations of one-nucleon spectroscopic overlaps for asymmetric parent nuclei, ^{14,16,22,24,28}O showed that SFs calculated with a microscopic coupled cluster model are quenched relatively to the simple SM ones, the quenching being particularly important for the nucleon knockout of the deficient species in strongly asymmetric nuclei [7]. On the other side, a weak dependence of this quenching on the nucleon binding was found [3].

Conflicting results did follow from this vast theoretical and experimental work. The variety of models, methods and energy regimes makes it difficult to extract a consistent explanation of the inadequacy of simple SMs to describe nuclear structure and to evaluate the importance and nature of the correlations. A consistent analysis of available experimental data, for all open reaction channels as well as different probes, with state-of-the art theory is lacking and of utmost importance for the understanding of nuclear structure along the nuclear landscape. Furthermore, it is essential to meet the challenges of new experimental developments and multiphysics research [26].

In this letter our goal is to contribute to a unified theoretical approach built on state-of-the-art *ab initio* Quantum Monte Carlo (QMC) wave functions [1], which can be used as a common input to transfer and nucleon knockout reactions with electron and nuclear probes. These QMC wave functions have been used to interpret successfully transfer reactions [21] and (e,e'p) experimental data [12]. We aim to shed light on the inadequacy of a simple (with an inert core) SM that exhausts the Spectroscopic Factor sum rule in a small space to describe (p,pN) reactions and to provide an understanding of (i) the ratios R_S, (ii) the ratios between the QMC and SM theoretical cross sections, R_σ, (iii) their relation with the corresponding ratios between the spectroscopic factors, R_Σ, and (iv) their correlation with the separation energy of the knocked out nucleon and other features of nuclei. We also aim (v) to test, for the first time, the ability of QMC wave functions to describe (p,pN) reactions. Our analysis of (p,pN) reactions with light nuclei will contribute to the construction of a unified interpretation of nucleon knockout reactions along the nuclear landscape, including the (p,pN) experimental data collected at the R3B-LAND setup at GSI [19,20,27].

2. Formalism

In this paper, we assume the standard ansatz for the knockout reaction. The one-nucleon spectroscopic overlap, the key nuclear structure input, is defined as the inner product of the A parent nucleus wave function and the fully antisymmetrized A − 1 residual nucleus plus the knockout nucleon wave function, and is calculated from fully correlated QMC wave functions generated using the NN Argonne V18 and the NNN Urbana X (AV18+UX) potentials, with explicit charge-dependence and charge-asymmetry terms [2]. We consider Variational Monte Carlo (VMC) overlaps for p- and n-knockout from ^{9}Li, ^{10}Be and ^{12}C nuclei. We use improved shell-model-like VMC wave functions for ^{12}C recently employed in benchmark calculations of neutrinoless double beta decay [28] and for ^{11}B in studies of nuclear charge radii of boron isotopes [29]. For ^{10}Be we have new shell-model-like VMC wave functions with additional spatial symmetry states beyond those used in studies of $B(E2)$ transitions in $A = 10$ nuclei [30,41]. Preliminary results with the Norfolk local chiral potential NV2+3-Ia* [42,43] show 5% variations in the SFs with respect to AV18+UX. The Green's Function Monte Carlo (GFMC) SFs for the ^{7}Li parent and residual ^{6}Li overlaps agree fairly well with the VMC ones, validating the use of VMC overlaps. We take the VMC and GFMC overlaps for the ^{7}Li parent nucleus from Ref. [24], which are able to describe the (e,e'p) reaction [12]. All QMC SFs are translationally invariant. Additionally, we have performed a convenient parameterization of the QMC overlaps using the procedure described in Ref. [24], which incorporates the adequate asymptotic behavior.

Table 1
Summary of the acronyms.

Quantity	Definition
$\Sigma(\mathcal{M})$	$\Sigma_i Z^i(\mathcal{M})$
R_Z	$Z^i(\text{QMC})/Z^i(\text{SM})\vert_{i=\text{g.s.}}$
R_Σ	$\Sigma(\text{QMC})/\Sigma(\text{SM})$
$\sigma_{\text{th}}(\mathcal{M})$	$\sum_i Z^i(\mathcal{M})\sigma^i_{\text{sp}}(\mathcal{M})$
R_σ	$\sigma_{\text{th}}(\text{QMC})/\sigma_{\text{th}}(\text{SM})$
R_S	$\sigma_{\text{exp}}/\sigma_{\text{th}}(\text{SM})$
$R_{\sigma\sigma}$	$R_\sigma[\sigma^i_{\text{sp}}(\text{WS})/\sigma^i_{\text{sp}}(\text{QMC})]\vert_{i=\text{g.s.}}$

We also take SFs from the simple SM of Cohen and Kurath (CK) [46], where only the (A-1)+N configuration is present in the parent nucleus state space, and all the valence nucleons are in p-shells in both parent and residual nuclei. In this model SFs are obtained from wave functions generated by diagonalizing the Hamiltonian in the nucleons valence space with effective two-body interactions, and require the well-known center of mass (c.m.) correction, given by $A/(A-1)$ [47].

The theoretical SFs for each structure model, $\mathcal{M}$, (QMC and simple SM) are denoted here as $Z^i(\mathcal{M})$, where i identifies the energy and the angular momentum of the residual nucleus, as well as the nucleon angular momentum channels, with the sum $\Sigma(\mathcal{M}) = \Sigma_i Z^i(\mathcal{M})$.

The one-nucleon overlaps normalized to unity are then used as initial-channel wave functions in the Faddeev/Alt-Grassberger-Sandhas (F/AGS) three-body reaction formalism [31,32] that provides single-particle cross sections $\sigma^i_{\text{sp}}(\mathcal{M})$. The theoretical inclusive cross section $\sigma_{\text{th}}(\mathcal{M})$ is obtained as the weighted sum $\sigma_{\text{th}}(\mathcal{M}) = \sum_i Z^i(\mathcal{M})\sigma^i_{\text{sp}}(\mathcal{M})$. These and other acronyms used in this manuscript are summarized in Table 1.

The F/AGS formalism allows a consistent and simultaneous treatment of all open channels, providing an exact solution of the three-body scattering problem for an assumed three-body Hamiltonian. This formalism includes all multiple scattering terms, contrary to other scattering frameworks that rely on assumed exact cancellations between multiple scattering terms [34]. It has been used recently in several exploratory studies of (p,pN) reactions [20,34–36] and it is able to model the experimental transverse momentum distributions [20,34].

We use the F/AGS in a non relativistic form since consistent treatment of relativistic kinematics and dynamics in Refs. [37,38] indicates only a small total relativistic effect for the total three-body breakup cross section, less than 10% in our energy regime of interest. However, separate relativistic effects may be quite sizable [37,38].

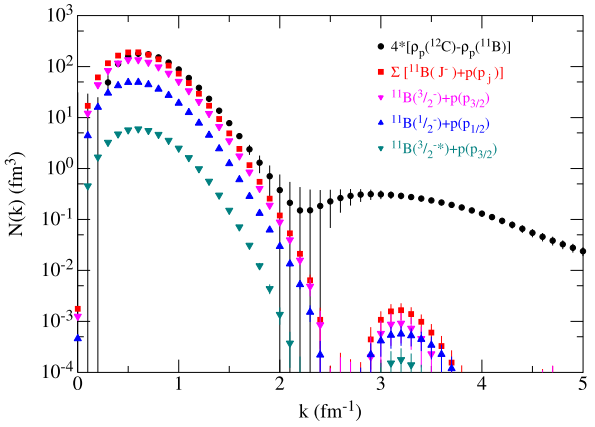

Fig. 1. VMC overlaps in momentum space $N(k)$ calculated for the low-lying states of ^{11}B. Also shown in black is the difference of ^{12}C and ^{11}B proton momentum distributions multiplied by 4 (the total number of protons in a p-shell in the Independent Particle Model).

The reaction formalism requires three pair interactions. We take the realistic NN AV18 potential for the proton-nucleon pair. For the interaction between nucleons and the residual nucleus we consider the Koning-Delaroche (KD) optical potential parameterization [39] used in preliminary calculations [36] and the Cooper potential [40] for ^{12}C, a global parameterization developed for medium-heavy nuclei and in particular for A = 12, that reproduce the elastic scattering data. From comparison with other parameterizations provided in [34] we estimate the uncertainty of the cross sections associated with optical parameterizations to be about 15%.

3. Results

We start by evaluating the one-nucleon spectroscopic overlaps for the parent nucleus ^{12}C, for which there are experimental (p,2p) data at 400 MeV/u [27]. The overlaps in momentum space are represented in Fig. 1, along with the difference between the VMC ^{12}C and ^{11}B proton momentum distributions. This difference exhibits a significant high-momentum tail, where about 15% of the protons have momenta above 1.4 fm^{-1}, unaccountable in any simple SM. The result for ^{12}C, shown here for the first time, is consistent with high-momentum electron scattering analysis [13], supporting the VMC wave function from which both momentum distributions and spectroscopic overlaps are generated and, therefore, corroborating our nuclear structure model. Interesting to say that the dominant source of this high momentum tail is the NN tensor force, coming from the one-pion-exchange potential, with a further significant contribution from the NNN force with its two-pion-exchange terms.

Using the Cooper potential we have obtained the total theoretical cross section $\sigma_{\rm th}(\text{QMC}) = 21.617$ mb with a ratio to the experimental value [27] of $\sigma_{\rm exp}/\sigma_{\rm th}(\text{QMC}) = 0.888(10)$. The experimental SFs, $Z^i_{\rm exp}$, are calculated dividing the (p,2p) experimental cross sections of Ref. [27] by $\sigma^i_{\rm sp}(\text{QMC})$. These SFs, together with those extracted from (p,2p) analysis of Ref. [27], electron scattering and transfer reactions [15], and their corresponding sums, are collected in Table 2. Our extracted spectroscopic factors differ by about 10% from those obtained by the Distorted Wave Impulse Approximation (DWIA) analysis of Ref. [27], which might be attributed to expected sensitivities of the single particle cross sections to the optical potential parametrizations, and in addition to possible reaction formalism effects.

Also shown in Table 2 are the theoretical VMC and SM (before the $A/(A-1)$ c.m. correction) SFs and their sums, $\Sigma(\mathcal{M})$.

Table 2
SFs for different low lying final states of ^{11}B.

Analysis	SF($3/2^-$)	SF($1/2^-$)	SF($3/2^-_2$)	Σ
QMC	$2.357_{(12)}$	$0.868_{(4)}$	$0.108_{(1)}$	$3.33_{(2)}$
SM [46]	2.85	0.75	0.38	3.98
(p,2p)	$2.43_{(28)}$	$0.29_{(03)}$	$0.24_{(03)}$	$2.96_{(28)}$
(e,e'p) transfer [15]	$1.72_{(11)}$	$0.26_{(2)}$	$0.20_{(2)}$	$2.18_{(15)[1.00]}$
(p,2p) [27]	$2.11_{(24)[0.82]}$	$0.26_{(3)[0.10]}$	$0.21_{(3)[0.08]}$	$2.58_{(30)[1.00]}$

It is found that the VMC spectroscopic strength appears to be distributed among the low lying states differently than the deduced experimental values, the sum of the SFs for the two $3/2^-$ states being relatively close to the experimental value and the $1/2^-$ state about three times larger than the available experimental values, a feature also common to the SF prediction of Cohen and Kurath [46]. The first excited $1/2^-$ state has a high excited state companion sitting at more than 10 MeV and this split should not account for the large theoretical SF. It remains unclear from the structure point of view, why theoretical and experimental SFs for the $1/2^-$ excited state differ significantly.

We also note that the sum of the SFs taken from CK is very close to the sum of particles in the shell (before c.m. correction), the well known sum rule. This results from the truncation of the nuclear state space, which assigns to one the probability of finding all valence nucleons in p-shells in parent and residual nuclei and the $(A-1)+N$ configuration in the parent nucleus. As a consequence, the sum of the CK SFs exhausts the sum rule. In contrast, the QMC overlaps are calculated from fully microscopic correlated wave functions for parent and residual nuclei, both normalized to one. This means that the states corresponding to the valence p-shell nucleons and to the $(A-1)+N$ partitions do not span the parent nucleus space. Accordingly, the sum rule, which should be obeyed by any good many-body theory, is not exhausted by the QMC SFs within the p-shell, but has significant contributions from a broader interval of states, including states in the continuum. This is partially reflected in the high-momentum tail of the proton distribution difference shown in Fig. 1.

In Table 3, for the ground-state parent and residual nuclei we compare experimental values of the point proton rms radii (r_p) [44,45] with the ones obtained from the QMC wave functions. For all the studied nuclei, including ^{12}C, we find quite a good agreement, validating the QMC approach. In addition, we present point neutron r_n and matter $r_m = [(Zr_p^2 + Nr_n^2)/A]^{1/2}$ radii, difference between the removed nucleon rms radius in the parent and residual nuclei, $\Delta r_N = r_N(A) - r_N(A-1)$, in the corresponding (p,pN) reaction, and the SF ratio $R_Z = Z^i(\text{QMC})/Z^i(\text{SM})$ with i being the ground state here.

The theoretical VMC and SM sums $\Sigma(\mathcal{M})$ and their ratios R_Σ (including c.m. correction) for all the studied nuclei are collected in Table 4. The ratios R_Σ range from 0.6 to 0.8 being consistent with Ref. [8]. This reduction is due to the fact that the simple SM SFs before the c.m. correction exhaust the sum rule, as discussed above, meaning that they are necessarily larger than the QMC ones, with an additional SM enhancement due to the c.m. correction $A/(A-1)$. This conclusion is independent of the interaction models. Also listed in the same Table are the results of partial sums over the final states of the residual nucleus below its breakup threshold, indicated as BPT (below particle threshold). The ratios of partial SF sums, shown also in the upper panel of Fig. 2, differ significantly from those of total SF sums, ranging from 0.5 to 1, which follows naturally from the fact that the spectroscopic strength is distributed among the states differently in the VMC and SM formalisms. The R_Σ BPT exhibit a moderate dependence on S_N, for the considered small asymmetry $(N-Z) \leq 3$. Nevertheless, the ratio R_Σ is always smaller for the knockout of the more correlated

Table 3
Radii, nucleon separation energies and QMC/SM SF ratios for the ground states of the parent ^{A}X and residual nucleus $^{A-1}$Y.

^{A}X	$^{A-1}$Y	J^{π}	S_N (MeV) exp	r_p (fm) QMC	r_n (fm) QMC	r_m (fm) QMC	r_p (fm) exp	Δr_N (fm) QMC	R_Z SF g.s.
^{7}Li		$3/2^-$		2.26	2.41	2.35	2.31(5)		
	^{6}Li	1^+	7.25	2.46	2.46	2.46	2.45(4)	−0.05	0.81
	^{6}He	0^+	9.97	1.94	2.82	2.53	1.92(1)	0.32	0.56
^{9}Li		$3/2^-$		2.07	2.45	2.33	2.11(5)		
	^{8}Li	2^+	4.06	2.13	2.44	2.33	2.20(5)	0.01	0.96
	^{8}He	0^+	13.94	1.83	2.79	2.58	1.84(2)	0.24	0.67
^{10}Be		0^+		2.28	2.46	2.39	2.22(3)		
	^{9}Be	$3/2^-$	6.81	2.36	2.46	2.42	2.36(1)	0.00	0.84
	^{9}Li	$3/2^-$	19.64	2.07	2.45	2.33	2.11(5)	0.21	0.58
^{12}C		0^+		2.37	2.37	2.37	2.32(1)		
	^{11}C	$3/2^-$	18.72	2.41	2.35	2.38	–	0.02	0.76
	^{11}B	$3/2^-$	15.96	2.35	2.41	2.38	2.28(13)	0.02	0.76

Table 4
Total and BPT sums of SFs, Σ, and ratios R_Σ. The SM* includes c.m. correction factors.

^{A}X	$^{A-1}$Y		Σ($\mathcal{M}$) SM	Σ($\mathcal{M}$) QMC	R_Σ QMC/SM*
^{7}Li	^{6}Li	BPT	1.016	0.874(3)	0.737(2)
			1.999	1.606(10)	0.689(4)
	^{6}He	BPT	0.592	0.389(1)	0.563(1)
			0.997	0.733(3)	0.630(2)
^{9}Li	^{8}Li	BPT	1.313	1.428(4)	0.967(3)
			3.859	3.597(14)	0.829(3)
	^{8}He	BPT	0.847	0.635(2)	0.666(2)
			1.000	0.785(3)	0.698(3)
^{10}Be	^{9}Be	BPT	2.356	2.214(9)	0.846(3)
			3.990	3.608(15)	0.814(3)
	^{9}Li	BPT	1.990	1.595(6)	0.721(3)
			1.990	1.680(6)	0.760(3)
^{12}C	^{11}C	BPT	3.980	3.326(17)	0.766(16)
			3.980	3.326(17)	0.766(16)
	^{11}B	BPT	3.980	3.333(17)	0.768(16)
			3.980	3.333(17)	0.768(16)

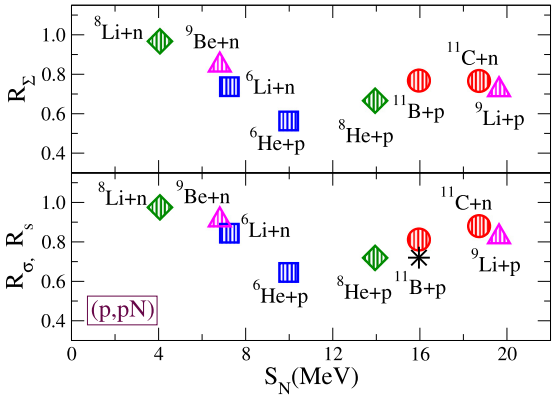

Fig. 2. Theoretical ratios (QMC/SM) of SF sums (upper panel) and (p,pN) cross sections (lower panel) restricted to final states below particle threshold (BPT) of the residual nucleus and quenching factors, R_S (asterisk), as functions of the nucleon separation energy.

deficient species nucleon, the proton in these cases, in accordance with previous findings [7,17].

On the other hand, the overlaps and consequently the SFs, as well as their VMC/SM ratios, are expected to be determined not solely by the separation energy S_N of the knockout nucleon but by its interplay with other features of nuclei. We consider the difference between the removed nucleon rms radius in the parent and the residual nuclei, Δr_N. This interplay between S_N and Δr_N stems from the fact that the radii difference indicates the actual overlaps of the nuclei wave functions, and the separation energy determines the fall of the overlap tail. The VMC and SM predict slightly different S_N, for comparison they are mapped to the experimental value, and Δr_N predictions are taken from VMC. We use a simple linear combination of S_N and Δr_N to simulate the SFs ratios leaving the residual nucleus in ground state as $R_Z \approx aS_N + b|\Delta r_N| + c$. The parameters a, b, and c are determined from the fit using 8 data sets from Table 3 leading to $a = (-0.00999 \pm 0.00276)$ MeV^{-1}, $b = (-0.804 \pm 0.127)$ fm^{-1}, and $c = (0.950 \pm 0.036)$, with the uncertainties of 28%, 16%, and 4%, respectively. R_Z represented by this linear combination is shown as full symbols in Fig. 3. An ideal representation would correspond to the line of slope one, but the real data points are quite close to that line, exhibiting much more clear linear trend as compared to Fig. 2. This suggests a reasonable linear representation of the ratios R_Z and, therefore, at least for a limited set of studied nuclei, a mild dependence on S_N and $|\Delta r_N|$, with small contribution of higher-order nonlinear terms.

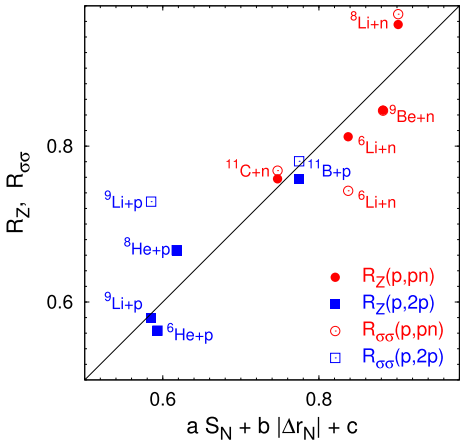

Fig. 3. QMC/SM ground state SF ratio R_Z and the renormalized BPT total cross section ratio $R_{\sigma\sigma}$ versus linear combination $aS_N + b|\Delta r_N| + c$ as described in the text.

In the limit of the knockout of a loosely bound, less correlated nucleon species, the separation energy is smaller and parent and residual nuclei have similar nucleon (removed species) radii, and thus small Δr_N. The dominant contribution to the SF comes from the tail of the overlap function, which is expected to be similar in the two models, leading to a ratio approaching one. In the linear representation this fact is reflected by the smallness of the first

Table 5
Single particle cross sections (in units of mb). The KD potential [39] is used for ^{7}Li, ^{9}Li, and ^{10}Be, the Cooper potential [40] for ^{12}C.

^{A}X	$^{A-1}$Y	J^{π}	σ_{sp}(WS)	σ_{sp}(QMC)
^{7}Li	^{6}Li	1^{+}	16.51	18.77
		0^{+}	15.49	18.01
	^{6}He	0^{+}	11.66	13.36
^{9}Li	^{8}Li	2^{+}	16.72	16.81
		1^{+}	16.21	16.46
	^{8}He	0^{+}	10.18	10.99
^{10}Be	^{9}Be	$3/2^{-}$	14.96	16.12
	^{9}Li	$3/2^{-}$	9.01	10.20
		$1/2^{-}$	8.80	10.45
^{12}C	^{11}C	$3/2^{-}$	7.80	8.92
		$1/2^{-}$	7.54	8.62
		$3/2^{-}_{2}$	7.15	8.18
	^{11}B	$3/2^{-}$	6.26	6.51
		$1/2^{-}$	5.95	6.46
		$3/2^{-}_{2}$	5.61	6.38

two terms, leaving $c = 0.950$ as the prevalent one, as shown in Fig. 3.

For the knockout of a deep, more correlated nucleon species, both the separation energy and Δr_N are larger, and the inner part of the overlap function has a greater impact due to the rapid fall of the functions. One expects the two models to differ in the inner overlap parts, sensitive to nuclear correlations, in particular, to short range ones. In the linear representation, the two first terms become competitive with the c term, leading to ratios smaller than one, as shown in Fig. 3.

We study now $R_\sigma = \sigma_{th}(\mathrm{QMC})/\sigma_{th}(\mathrm{SM})$. Observed weak sensitivity of the single particle cross section to the overlap functions justifies a simpler way to generate the initial bound-state wave functions for SM: in the given nucleon-core partial wave we take the Woods-Saxon potential with standard radius and depth adjusted to the separation energy of the removed nucleon; no antisymmetrization is considered. The corresponding single particle cross sections $\sigma^i_{sp}(\mathcal{M})$ calculated using one-nucleon overlap functions obtained from Woods-Saxon potentials and QMC wave functions, are collected in Table 5. Their ratios vary between 1.0 and 1.15 for ground state residual nuclei but may reach 1.19 for excited states. The small departure from 1.0 arises because the one-nucleon spectroscopic factors normalized to unit included in the evaluation of the single particle cross sections explore transfer momentum larger than zero, and the sp cross section explores regions slightly beyond zero transfer momentum. This indicates that the microscopic treatment of the overlaps for SFs has its biggest effect on the SFs, single particle cross sections being affected less. Additionally, we expect the ratios R_σ to be nearly independent of the choice of the optical potential parameterization. For the case of ^{12}C we verified the potential independence of these ratios since similar results are obtained with different parameterizations [40,39]. As a result of our ansatz, and since we are considering low-lying states of the residual nucleus and we found only weak dependence of $\sigma^i_{sp}(\mathcal{M})$ on S_N [35], we also expect R_σ BPT to be quite close to the corresponding R_Σ. This is confirmed when comparing the lower and upper panels of Fig. 2. The ratios R_σ BPT, range from 0.6 to 1, slightly enhanced due to $\sigma^i_{sp}(QMC) > \sigma^i_{sp}(WS)$, and exhibit a similar moderate dependence on S_N as R_Σ, the quenching being more significant for the knockout of the nucleon of the deficient species. These results are compatible with the behavior of the ratio R_S as a function of S_N found in Refs. [19,20] opening a path for an unified understanding of both light and medium light nuclei.

By the same token, the ratios R_Σ and R_σ BPT are also expected to be determined by a similar interplay between Δr_N and S_N for the case where transitions to the ground state are dominant. To have insight on this we also represent in Fig. 3 as open symbols the BPT ratio $R_{\sigma\sigma} = R_\sigma[\sigma^i_{sp}(WS)/\sigma^i_{sp}(QMC)]$ where i denotes the ground state; the factor $[\sigma^i_{sp}(WS)/\sigma^i_{sp}(QMC)]$ removes the enhancement of the QMC cross sections due to its slightly larger sp cross sections when compared to the WS ones, therefore evincing the effect of the SFs. In three of the eight cases considered only one state contributes to $R_{\sigma\sigma}$, making it identical to R_Z. Therefore, the points coincide. The deviation between the open and corresponding full symbols results when contributions of excited states show a different trend in QMC and SM as compared to the ground state. Examples are ^{9}Li+p or ^{6}Li+n. The linear representation as a function of both Δr_N and S_N, albeit with larger deviations than for R_Z, is an indication that the reaction mechanism does not probe exclusively the tail of the overlaps between the parent and residual nucleus. In addition, by the same physical arguments drawn for the SFs, we expect the quenching factors R_S to be smaller than unity, independently of the interaction models.

An analysis of nucleon removal has been performed using a formalism that considers the factorization of the cross section into SFs and sp cross sections [16,18]. However, in transfer reactions and in nucleon knockout reactions where both projectile and target are composite nuclei, the reaction mechanisms are substantially different from those of (p,pN) reactions, preventing the conclusion that the factorization is a reasonable approximation. We have reanalyzed the results of this analysis by taking their sp removal cross sections and the QMC and CK SFs presented here. We found that R_S are consistently smaller than R_σ, suggesting that both the factorization and the clean link between the R_Σ and R_σ, that exists for (p,pN) knockout reactions, are not expected to hold for the removal reactions [33]. Further work on this issue is desirable.

4. Conclusion

In conclusion, in the present letter we analyze, for the first time, (p,pN) reactions for $A \leq 12$ and $(N - Z) \leq 3$ using state-of-the art nuclear structure and three-body scattering formalisms, namely QMC wave functions and the F/AGS reaction theory. New QMC wave functions used to describe ^{12}C and ^{11}B nuclei yield results consistent with experimental data of proton point rms radius, (p,2p) total cross section at 400 MeV/u, as well as momentum distributions compatible with electron scattering data analysis.

We show the shortcomings of the SM to describe (p,pN) reactions due to the strong truncation of the state spaces of the nuclei. This leads necessarily to an overestimation of the cross sections, independently of the interaction models. Further, nontrivial structure effects have to be taken into account, through two- and three-body correlations incorporated in the wave functions, a characteristic of the fully correlated QMC wave functions.

The QMC/SM ground state SF ratio is found to be reasonably represented by a linear combination of separation energy and difference between the removed nucleon rms radius in the parent and residual nuclei. The ratio between the partial sums of QMC and SM cross sections, R_σ, is close to the ratio of the corresponding partial sums of SFs, R_Σ. Hence, one expects the quenching ratios to be determined by a delicate interplay between the radii of the parent and the residual nuclei and the nucleon separation energy, similar to the ratio of SFs. Last, R_Σ and R_σ show a moderate dependence on S_N and difference between the removed nucleon rms radius in the parent and residual nuclei, and are smaller for the knockout of the more correlated nucleon of the deficient species.

A consistent experimental program of transfer and knockout (with light and heavier targets) with proton and electron probes for $A \leq 12$ nuclei will be very useful to get further insight on the

shortcomings of the simplified SM picture and on the structure of light nuclei.

Acknowledgements

R.C., E.C., A.A., A.M., A.D. and R.B.W. are supported by Fundação para a Ciência e Tecnologia of Portugal, Grant No. PTD/FIS-NUC/2240/2014. A.D. is supported by the Alexander von Humboldt Foundation, Grant No. LTU-1185721-HFST-E. R.B.W. is supported by the US Department of Energy, Office of Nuclear Physics, contract No. DE-AC02-06CH11357 and the NUCLEI SciDAC program; computing time was provided by the Argonne Leadership Computing Facility under the INCITE program and the Argonne Laboratory Computing Resource Center. We thank B. Jonson, P. Diaz-Fernandez and A. Heinz for reading the manuscript.

Declaration of competing interest

The authors declare that they have no known competing financial interests or personal relationships that could have appeared to influence the work reported in this paper.

References

[1] R.B. Wiringa, et al., Phys. Rev. C 89 (2014) 024305.
[2] J. Carlson, et al., Rev. Mod. Phys. 87 (2015) 1067.
[3] C. Barbieri, W.H. Dickoff, Int. J. Mod. Phys. A 24 (2009) 2060.
[4] S. Quaglioni, P. Navratil, Phys. Rev. Lett. 101 (2008) 092501.
[5] N.K. Timofeyuk, Phys. Rev. C 88 (2013) 044315.
[6] F. Barranco, et al., Phys. Rev. Lett. 119 (2017) 082501.
[7] O. Jensen, et al., Phys. Rev. Lett. 107 (2011) 032501.
[8] V.R. Pandharipande, I. Sick, P.K.A. de Witt Huberts, Rev. Mod. Phys. 69 (1997) 981.
[9] L. Coraggio, A. Covello, A. Gargano, N. Itaco, T.T.S. Kuo, Prog. Part. Nucl. Phys. 62 (2008) 135.
[10] The CLAS Collaboration, Nature 560 (2018) 617.
[11] L. Lápikas, Nucl. Phys. A 553 (1993) 297.
[12] L. Lápikas, J. Wesseling, R.B. Wiringa, Phys. Rev. Lett. 82 (2009) 4404.
[13] D. Rohe, et al., Phys. Rev. Lett. 93 (2004) 182501.
[14] R. Subedi, et al., Science 320 (2009) 1475.
[15] G.J. Kramer, H.P. Block, L. Lapikas, Nucl. Phys. A 679 (2001) 267.
[16] B.A. Brown, et al., Phys. Rev. C 65 (2002) 061601(R).
[17] J.A. Tostevin, A. Gade, Phys. Rev. C 90 (2014) 057602.
[18] G.F. Grinyer, et al., Phys. Rev. C 86 (2012) 024315.
[19] L. Atar, et al., Phys. Rev. Lett. 120 (2018) 052501.
[20] P. Díaz Fernández, et al., Phys. Rev. C 97 (2018) 024311.
[21] K.M. Nollett, R.B. Wiringa, Phys. Rev. C 83 (2011) 0410001(R).
[22] J. Lee, et al., Phys. Rev. Lett. 104 (2010) 112701.
[23] F. Flavigny, et al., Phys. Rev. Lett. 110 (2013) 122503.
[24] I. Brida, Steven C. Pieper, R.B. Wiringa, Phys. Rev. C 84 (2011) 024319.
[25] M. Gómez-Ramos, A.M. Moro, Phys. Lett. B 785 (2018) 511.
[26] P.F. Bortignon, R.A. Broglia, Eur. Phys. J. A 52 (2016) 64.
[27] V. Panin, et al., Phys. Lett. B 753 (2016) 204.
[28] X.B. Wang, et al., Phys. Lett. B 798 (2019) 134974.
[29] B. Maab, et al., Phys. Rev. Lett. 122 (2019) 182501.
[30] E.A. McCutchan, et al., Phys. Rev. C 86 (2012) 014312.
[31] L.D. Faddeev, Zh. Eksp. Teor. Fiz. 39 (1960) 1459.
[32] E.O. Alt, P. Grassberger, W. Sandhas, Nucl. Phys. B 2 (1967) 167.
[33] A. Deltuva, Phys. Rev. C 99 (2019) 024613.
[34] R. Crespo, E. Cravo, A. Deltuva, Phys. Rev. C 99 (2019) 054622.
[35] E. Cravo, R. Crespo, A. Deltuva, Phys. Rev. C 93 (2016) 054612.
[36] R. Crespo, et al., Inst. Phys. Conf. Ser. 966 (2018) 012056.
[37] H. Witala, J. Golak, R. Skibinski, Phys. Lett. B 634 (2006) 374.
[38] H. Witala, et al., Few-Body Syst. 49 (1–4) (2011) 61–64.
[39] A.J. Koning, J.P. Delaroche, Nucl. Phys. A 713 (2003) 231.
[40] E.D. Cooper, et al., Phys. Rev. C 47 (1993) 297.
[41] R.B. Wiringa, Phys. Rev. C 73 (2006) 034317.
[42] M. Piarulli, et al., Phys. Rev. Lett. 120 (2018) 052503.
[43] M. Baroni, et al., Phys. Rev. C 98 (2018) 044003.
[44] H. De Vries, C.W. De Jager, C. De Vries, At. Data Nucl. Data Tables 36 (1987) 495.
[45] Z.-T. Lu, et al., Rev. Mod. Phys. 85 (2013) 1383.
[46] S. Cohen, D. Kurath, Nucl. Phys. A 101 (1967) 1;
D. Kurath, private communication.
[47] A.E.L. Dieperink, T. de Forest Jr., Phys. Rev. C 10 (1974) 543.